Design Status of the CLIC Beam Delivery System

M. Aleksa, R. Assmann, H. Burkhardt, S. Redaelli*, T. Risselada, S. Russenschuck, D. Schulte, F. Zimmermann, CERN, Geneva, Switzerland; A. Faus-Golfe, IFIC, Valencia, Spain; G.A. Blair, Royal Holloway, London, UK

Abstract

Recent developments on the CLIC collimation and final focus are described. The combination of a shortened linear, or alternative nonlinear, collimation section and a compact final focus substantially reduces the overall system length at 3 TeV centre-or-mass energy to less than 3 km. A beam-delivery system (BDS) for 500 GeV centre-of-mass energy is obtained by relatively minor optics modifications of the 3-TeV system . It promises a satisfactory performance. The attainable luminosity can be raised, at both energies, by decreasing the beta functions at the collision point. We also discuss field errors, gas scattering and wake fields in the final quadrupoles, and the collimation parameters.

1 INTRODUCTION

Designs of a baseline collimation and compact final focus for CLIC at 3 TeV were reported in Refs. [1] and [2]. Here we describe new developments, which include a substantial shortening of the collimation system, an optics design and performance evaluation for 500 GeV, and an alternative nonlinear collimation system. Table 1 summarizes the beam and final-focus parameters for the nominal 3 TeV centre-of-mass (cm) energy and for 500 GeV. The beta functions at the interaction point (IP) are somewhat variable. Their optimum is determined by integrated simulations [3, 4] modelling the beam transport from the start of the linac to the IP, including the beam-beam collision.

In the following, we describe recent changes to the 3-TeV optics and the optics modifications for 500 GeV. We then discuss a few aspects related to the final quadrupole and the interaction region (IR). We conclude by summarizing important design issues for the collimation system.

2 OPTICS

The CLIC beam-delivery optics for 3 TeV is depicted in Fig. 1. The total length is 2.5 km per side. Compared with an earlier layout [2], the collimation system was considerably shortened. This was achieved by rescaling the system parameters (*i.e.*, length and bending angles) and by omitting half of the energy collimation. Thereby, we accepted a larger emittance growth from synchrotron radiation, resulting in a luminosity decrease by about 10%. We also possibly sacrificed collimation efficiency and machine protection.

In the previous baseline optics [2] the length of the energy collimation section had been scaled by a factor 8 and the bending angles by a factor 1/32 with respect to the 1 TeV NLC design [6]. For the new shorter system the scaling factors chosen are 5 and 1/12 respectively. As a consequence the I_5 radiation integral [9] has increased from 1.8×10^{-20} m to 1.9×10^{-19} m. The new number corresponds to an emittance growth of $\Delta(\gamma\epsilon_x) \approx$

Table 1: Final-focus (FF), collimation system (CS), and beam parameters at 3 TeV and 500 GeV cm energy. Emittance numbers refer to the entrance of the BDS. Shown in parentheses are earlier values [5, 1, 2], illustrating the evolution of the design.

parameter	symbol	3 TeV	500 GeV
FF length [km]		0.5 (3.1)	0.5
CS length [km]		2.0 (5.8)	2.0
BDS length [km]		2.5 (8.9)	2.5
hor. emittance [μm]	$\gamma\epsilon_x$	0.68	2.0
vert. emittance [nm]	$\gamma\epsilon_y$	10 (20)	10
hor. beta function	β_x^*	6.0	3
[mm]		(8)	
vert. beta function	β_y^*	0.07	0.05
[mm]		(0.15)	
spot size [nm]	$\sigma_{x,y}^*$	67, 2.1	180, 4.2
bunch length [μm]	σ_z^*	35 (30)	35
IP free length	l^*	4.3 (2.0)	4.3
crossing angle [mrad]	θ_c	20	20
lum. w/o pinch	L_0	4.0	1.9
[10^{34} cm^{-2}s^{-1}]			

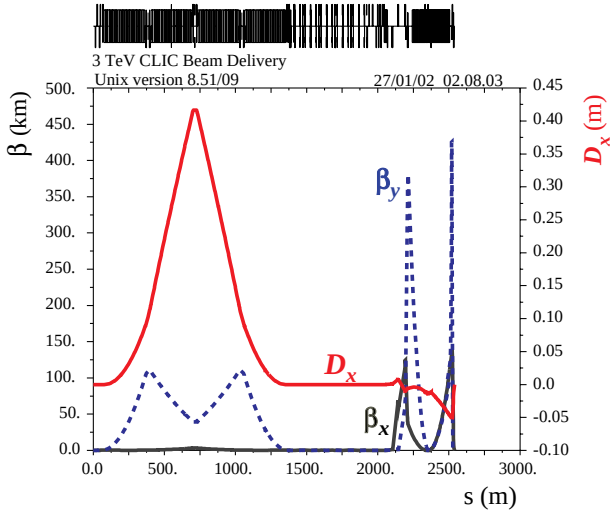

Figure 1: BDS optics at 3 TeV; $\beta_x^* = 6$ mm, $\beta_y^* = 70$ μm.

* PhD student of the University of Lausanne, Institut de Physique des Hautes Energies (IPHE), Switzerland.

$(4 \times 10^{-8}\ \mathrm{m}^2\ \mathrm{GeV}^{-6})E^6 I_5 \approx 0.09\ \mu$m, which is near the tolerable limit.

The compact final focus is a design developed by P. Raimondi, which is based on nonzero dispersion across the final doublet [7]. Its application to CLIC was described in Ref. [1], We more recently reduced the IP beta functions in both planes, down to $\beta_x^* \approx 6-7$ mm, and $\beta_y^* \approx 70-80\ \mu$m (previously 8 mm and 150 μm). At 3 TeV the reduction in $\beta_{x,y}^*$ increases the luminosity by 10–20%, as illustrated in Fig. 2. We here benefit from the short rms bunch length in CLIC, which is only 35 μm, *i.e.*, still much smaller than β_y^*. Simulations including beam-beam collisions show that at 3 TeV the luminosity gained by reducing the beta functions roughly compensates the loss from shortening the collimation system. However, further reductions of the IP beta functions are prevented by a steep spot size increase due to the Oide effect [8].

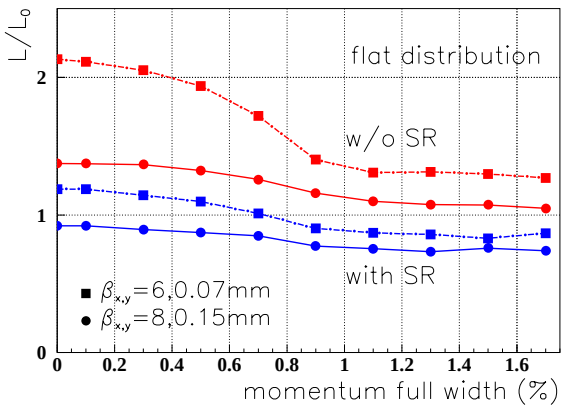

Figure 2: Relative luminosity w/o pinch vs. full-width momentum spread at 3 TeV, as simulated by upgraded MAD [10] (cross-checked with PTC [11]), for two different values of $\beta_{x,y}^*$ and $\gamma\epsilon_y = 10$ nm ($L_0 = 4.6 \times 10^{34}$ cm^{-2}s^{-1}).

The free length between the final quadrupole and the IP is large $l^* = 4.3$ m, as for NLC [7]. We consider it a major advantage of the compact final focus that the final quadrupole can be positioned outside of the detector solenoid and its fringe.

The optics for 500 GeV is obtained by minor modifications to the 3-TeV system. The total system length is the same, but the bending angles and the dispersion function in the final focus are 4.25 times larger than at 3 TeV (the sextupole fields are correspondingly reduced). In the energy collimation section, the bending angles and dispersion are also increased, but only by 20%. Because the Oide effect is much weaker at 500 GeV, the beta functions at the IP can be squeezed further, down to values as small as $\beta_x^* = 3$ mm, and $\beta_y^* = 50\ \mu$m. Note that the IP distribution then becomes distinctly non-Gaussian and the rms beam size is no longer a good indication of the luminosity. Table 2 shows that, in the tracking simulation, for constant emittances at the entrance of the final focus, the geometric luminosity without pinch increases from $L = 1.02 \times 10^{34}$ cm^{-2} s^{-1} for $\beta_y^* = 150\ \mu$m, $\beta_x^* = 10$ mm, to $L = 1.85 \times 10^{34}$ cm^{-2} s^{-1} for $\beta_y^* = 50\ \mu$m, $\beta_x^* = 3$ mm (at 200 Hz with $\gamma\epsilon_y = 10$ nm). This is almost twice the desired target value. The luminosity with pinch is inferred from integrated simulations [3, 4], which show that reducing only β_y^* and leaving β_x^* at 10 mm preserves the quality of the luminosity spectrum.

Table 2: Effect of varying $\beta_{x,y}^*$ at 500 GeV on the rms spot sizes $\sigma_{x,y}$ and the luminosity without pinch for a 200-Hz repetition rate, $n_b = 154$ bunches/train, and $N_b = 4 \times 10^9$. When reducing $\beta_{x,y}^*$, the rms spot size no longer reflects the effective beam size which determines the luminosity.

$\gamma\epsilon_y$ [nm]	β_y^* [μm]	β_x^* [mm]	σ_x [nm]	σ_y [nm]	L [10^{33} cm^{-2} s^{-1}]
20	150	10	209	2.65	7.3
10	150	10	209	1.88	10.2
10	110	10	209	1.69	11.5
10	70	10	209	1.55	13.6
10	50	10	209	1.56	15.0
10	50	8	189	1.77	16.0
10	50	6	169	2.17	17.2
10	50	4	160	3.12	18.1
10	50	3	178	4.07	18.5

3 FINAL QUADRUPOLE ISSUES

Two final quadrupoles based on the permanent-magnet material Sm_2Co_{17} have been designed using the ROXIE program [12]. The stronger magnet achieves a gradient of 467.5 T/m, the other the nominal gradient of 388 T/m [12] required by the present optics. Much weaker magnets would be needed at 500 GeV. We assume that the permanent-magnet field cannot be varied and that fine tuning of the IP beta functions is done using upstream quadrupoles. Table 3 lists relative harmonic field errors for the preliminary design of the two permanent-magnet quadrupoles and for one of the chromatic correction sextupoles [12]. If the nth order multipole error b_n of a quadrupole remains uncompensated, the vertical spot size increases by

$$\frac{\Delta\sigma_y^*}{\sigma_{y0}^*} \approx (n-1)\sqrt{(2n-5)!!}\,\frac{GL_Q b_n}{(B\rho)r_0^{n-2}}\,\beta_{Q,x}^{\frac{n-2}{2}}\,\epsilon_x^{\frac{n-2}{2}}\,\beta_{Q,y}\ ,$$

where $\beta_{Q,x(y)}$ denotes the horizontal (vertical) beta function at the center of the magnet, L_Q is the magnet length, G the gradient in T/m, and $(B\rho)$ the magnetic rigidity. Inserting the values of Table 3 the beams-size blow up from the quadrupole b_4 field errors is less than 0.06% and that from the sextupole b_5 error about 0.01%.

The beam-pipe radius in the final quadrupoles is small (3.8 mm at the minimum), in order to produce the desired gradient. Therefore, resistive-wall wake fields become a concern. The centroid deflection due to the resistive wall is

$$\langle \Delta y' \rangle = 0.3\,\frac{2}{\pi}\,\frac{r_e N_b L}{a^3\gamma}\,\left(\frac{c}{\sigma\sigma_z}\right)^{1/2}\langle y \rangle\ ,$$

Table 3: Relative harmonic field errors for 16-segment quadrupoles and 24-segment sextupoles at $r_0 = 2.2$ mm in units of 10^{-4}, with 1 mm stainless steel support pipe.

	quad. 1	quad. 2	sext.
strength	467.5 T/m	398.2T/m	90kT/m^2
b4	0.035	0.0003	
b5			0.446
b6	0.109	-0.323	
b7			0.519
b8	-0.002	-0.0001	

where a is the radial aperture, σ the conductivity in s^{-1}, and the factor 0.3 arises from averaging over the longitudinal bunch distribution. A figure of merit is the jitter enhancement K, given by

$$K \equiv \frac{\langle \Delta y' \rangle / \sigma_{y'}}{\langle y \rangle / \sigma_y} = 0.3 \frac{2}{\pi} \frac{r_e N_b L}{a^3 \gamma} \left(\frac{c}{\sigma \sigma_z} \right)^{1/2} \beta_y \ .$$

As an example, considering $\sigma = 5.4 \times 10^{17}$ s^{-1} (Cu), $a = 3.3$ mm, $E = 1.5$ TeV, $N = 4 \times 10^9$, $\sigma_z = 30$ μm, a length $L = 10$ m, $\beta_y = 400$ km, we find $K = 0.31$ (or a 5% enhancement if motion in y and y' is uncorrelated).

The small chamber apertures might also compromise the pumping speed, possibly degrading the vacuum pressure. Local pumping may be accomplished either by using segments of permanent material with intermediate space, by a long slit along the magnet, or by coating with getter material. To estimate the effect of the residual gas, we assume a train consisting of 154 bunches, each containing 4×10^9 electrons, which passes through 5 m of carbon monoxide gas at a pressure of 10 nTorr. The dominant scattering process is bremsstrahlung, with a cross section of 6.5 barn for an energy loss larger than 1% [14]. This yields 0.6 scattering events per bunch train.

4 COLLIMATION

The transverse beam halo must be collimated in order to ensure acceptable background in the detector. The transverse collimation depth is set by the requirement that the synchrotron-radiation fan generated in the final quadrupoles does not hit any aperture on the incoming side of the collision point. Leaving a margin of $2\sigma_x$ and $3\sigma_y$, respectively, the betatron collimation should be set to $\pm 12\sigma_x$ and $\pm 80\sigma_y$. The situation for the energy collimation is different. Here, the collimation requirements are imposed by failure modes in the linac. According to a detailed study [13] energy collimation at about $\pm 1.5\%$ will protect the downstream parts of the beam delivery system against all the linac failures considered, including the associated betatron oscillations. The collimator parameters that correspond to these collimation depths and to the optics shown in Fig. 1 are listed in Table 4. For the emittances of Table 1, the rms beam sizes at the energy spoiler are $\sigma_x \approx 756$ μm, $\sigma_y \approx 15$ μm, so that $\sigma_r \equiv \sqrt{\sigma_x \sigma_y} \approx 108$ μm. As far as spoiler survival in case of beam impact is concerned, this is rather marginal [15]. The spoiler is likely to be destroyed if the normalized vertical emittance is smaller than 10 nm.

Table 4: Collimator parameters at 3 TeV, assuming $\gamma\epsilon_x = 0.68$ μm, $\gamma\epsilon_y = 10$ nm, $\delta_{\rm rms} = 0.28\%$.

energy spoiler gap	± 4 mm
β_x spoiler gap	± 95 μm
β_y spoiler gap	± 104 μm
spoiler material	C (or Be)
spoiler length	177 mm (0.5 r.l.)
absorber material	Ti (Cu coated)
absorber length	712 mm (20 r.l.)
number of energy spoilers	1
number of β_x spoilers	4
number of β_y spoilers	4

As an alternative, we presently explore a nonlinear collimation system [16]. This system uses skew sextupoles to blow up the beam size at the spoiler. The main advantage of the nonlinear system is the larger beam size at the spoiler and, hence, better machine protection. In the current layout, the nonlinear system has about the same length as the linear system. Possible disadvantages include the existence of 'holes' in phase space where collimation is not effective.

5 REFERENCES

[1] F. Zimmermann, et al., "Final-Focus Schemes for CLIC at 3 TeV," Proc. HEACC'02, Tsukuba (2001).

[2] R. Assmann, et al., "Overview of the CLIC Collimation Design," PAC2001, Chicago (2001).

[3] R. Assmann et al., "CLIC Simulations from the Start of the Linac to the Interaction Point," this conference.

[4] D. Schulte, "Luminosity Limitations at the Multi-TeV Linear Collider Energy Frontier," this conference.

[5] F. Zimmermann, et al., "Final-Focus System for CLIC at 3 TeV", EPAC 2000 Vienna (2000)

[6] P. Tenenbaum, et al., "Studies of beam optics and scattering in the Next Linear Collider Postlinac Collimation System," LINAC 2000 Monterey (2000).

[7] P. Raimondi et al., PRL 86, 3779 (2001)

[8] K. Oide, PRL 61, 1713 (1988).

[9] R. Helm, et al., SLAC-PUB-1193 (1973).

[10] H. Grote and F. C. Iselin, CERN-SL-90-13-AP-REV.2.

[11] E. Forest and F. Schmidt, "Polymorphic Tracking Code."

[12] M. Aleksa, S. Russenschuck, CLIC Note 506 (2001).

[13] D. Schulte et al., "Failure Modes in CLIC," PAC2001, Chicago (2001).

[14] H. Burkhardt, Int. Workshop on Future e+e- Linear Colliders, Sitges 1999, CERN-SL-057-AP and CLIC Note 416.

[15] S. Fartoukh, et al., CERN-SL-2001-012 AP (2001).

[16] A. Faus-Golfe, et al., "A Nonlinear Collimation System for CLIC," this conference.